



A low velocity belt beneath northern and eastern Tibetan Plateau from Pn tomography

Chuntao Liang^{1,2} and Xiaodong Song¹

Received 28 August 2006; revised 6 October 2006; accepted 18 October 2006; published 22 November 2006.

[1] New Pn tomography on Tibetan Plateau (TP) and neighboring region is conducted with data assembled from various sources. The improved Pn tomographic image delineates several distinct geophysical regimes that are approximately separated by geological boundaries at surface. Dense distribution of the stations in the eastern half of the plateau allows us to infer a 3D view of crustal thickness variation of the region. The most striking feature is the bended low velocity belt (LVB), which extends from west to east beneath Qiangtang block and Songpan Ganzi fold belt (SGFB) in northern TP and then turns consistently southward with SGFB beneath eastern TP and further south to Indo-China. The consistency between geological boundaries on surface and sharp velocity contrast boundaries in uppermost mantle may suggest strong deformation coupling between crust and, at least uppermost mantle, if not whole lithosphere. A north-south striking LVB is also observed cutting through the southern TP, coinciding with the Yadong-Gulu rift at surface. Our tomographic results are generally consistent with dynamic models that involve with underthrusting in the southern TP, shortening in the northern TP, and extrusion to the east and the southeast. Furthermore, our results suggest significant east-west variations in the structure and dynamics. **Citation:** Liang, C., and X. Song (2006), A low velocity belt beneath northern and eastern Tibetan Plateau from Pn tomography, *Geophys. Res. Lett.*, *33*, L22306, doi:10.1029/2006GL027926.

1. Introduction

[2] It is well recognized that the rising of the Tibetan Plateau (TP) is a result of the ongoing collision of the India Plate and the Eurasia Plate (Figure 1). However, some basic issues regarding the deformation distribution and the TP uplifting mechanisms are still uncertain [Yin and Harrison, 2000; Johnson, 2002]. Apparently, detailed imaging of the sub-surface 3D structure of the crust and lithosphere provides a key to understand the orogenic processes. Unfortunately, sparse distribution of seismic stations in the region has greatly hindered this effort. Most previous seismological studies, including surface wave inversions and body-wave travel-time and waveform studies, have relied upon a few stations from global data sets. The resolution is poor, making it difficult to relate the

seismic parameters to geological structures. Over the last decade, a number of arrays of temporary seismic stations have been deployed in selected areas of Tibet or Tien Shan. They have provided unprecedented resolution of the crust and upper mantle beneath the TP, although these studies are restricted to certain linear profiles or small areas.

[3] One of the best-documented features from years of geophysical investigation is the contrast in physical properties at depth between northern and southern TP, despite remarkably uniform topography of the plateau. The observed features include: Upper mantle P and S velocities are low in the north and high and shield-like in the south [Chen and Molnar, 1981; Holt and Wallace, 1990; Rodgers and Schwartz, 1998]; Sn propagation is inefficient in the north and efficient in the south [Barazangi and Ni, 1982; McNamara et al., 1995; Rapine et al., 1997]; Shear-wave splitting is strong in the north and weak in the south [McNamara et al., 1994; Sandvol et al., 1997; Chen and Ozalaybey, 1998; Huang et al., 2000]; Pn velocity is low in the north and high in the south [Zhao and Xie, 1993; McNamara et al., 1997; Liang et al., 2004; Hearn et al., 2004; Sun and Toksöz, 2006]. These observations have provided important constraints on dynamics models of the TP [e.g., Owens and Zandt, 1997; Huang et al., 2000; Johnson, 2002].

[4] In this study, we present tomographic inversion results for the TP and surrounding regions using a large collection of Pn travel times acquired from various sources (see auxiliary material¹ Figure S1). Our recent tomographic inversions of the whole China have shown major features that correlate with surface geology [Liang et al., 2004]. However, the resolution in the TP is the poorest. Our study area was selected intentionally to cover the Himalaya and the TP as well as the surrounding regions. Almost all regional studies so far have been based on data collected solely within the TP. However, the structures beneath the surrounding regions, which provide a boundary condition of the interactions between the India and Eurasia plates, are as important as that beneath the plateau itself to investigate its dynamics and evolution. Dynamic models proposed previously, for example, have based on the assumption that the low velocity zone is localized in northern plateau [e.g., Owens and Zandt, 1997; Huang et al., 2000; Johnson, 2002]. Our results show that the low velocity in northern Tibet extends to eastern margin and southeastern margin to form a distinct low velocity belt (LVB). The relatively dense distribution of the stations in the eastern half of the plateau allows us to infer a 3D view of crustal thickness variation of

¹Department of Geology, University of Illinois at Urbana-Champaign, Urbana, Illinois, USA.

²Now at Center for Earthquake Research and Information, University of Memphis, Memphis, Tennessee, USA.

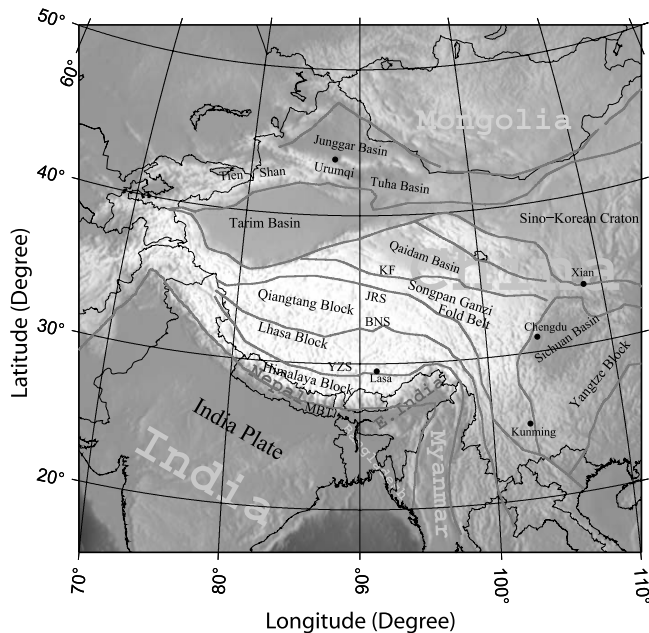


Figure 1. Major tectonic blocks of the Tibetan Plateau and surrounding region.

the region. We will discuss tectonic implications of these results.

2. Data and Methods

[5] Our data come from five sources: (1) Chinese national bulletins (Annual Bulletins of Chinese Earthquakes), (2) Chinese regional bulletins (from Yunnan and Sichuan Seismological Bureaus), (3) international bulletins (from the International Seismological Center), (4) hand-picked data from three temporary seismic arrays deployed in the TP: joint Sino-US research project (1991–1992) [Owens *et al.*, 1993], INDEPTH-II and INDEPTH-III [Nelson, 1996], and (5) hand-picked data from a few newly installed Chinese digital broadband seismic stations in TP. Most of the data from the first three data sets came from our previous study for the whole Chinese continent [Liang *et al.*, 2004]. The last two datasets (which added over 1200 new rays) are especially important to increase the ray and station coverage inside TP.

[6] We generally follow the data selection criteria described in Liang *et al.* [2004] except that: (1) the minimum ray distance is increased from 2° to 3° to make sure a clear separation of Pn and Pg because of the thick crust; (2) we substitute the ISC source location with the EHB [Engdahl *et al.*, 1998] source location if the latter is available; and (4) we also modified the earthquake grouping technique described in the appendix of Liang *et al.* [2004], which serves to locate earthquake clusters. We use the average of all earthquake locations in one cluster as the center of this cluster. If one station records more than one earthquake in the cluster, their residuals (corresponding to 1-D model) are averaged to be the residual of this station relative to the cluster center. This procedure partially averages out the noise in the original data and reduces greatly the unevenness of data distribution but still keeps the

overall ray coverage intact. In this study, we group earthquakes into a cluster within a radius of 8 km.

[7] After applying the above selection criteria, we finally obtained 44018 rays from 3585 clusters and 272 stations. This number is about 30 times of the dataset used in previous study of McNamara *et al.* [1997] and more than 100 times of Zhao and Xie [1993]. With the average crust velocity 6.3 km/s, we obtain the average Pn velocity about 8.06 km/s and average crust thickness of 51 km.

[8] We adopt the inversion scheme from Hearn [1996]. We divide the study area into 2-D cells with the size of 0.5° by 0.5° . Inversion yields Pn velocity in every cell, and time delays for each station and earthquake. Details of implementations of inversion, regularization and resolution tests are described by Liang *et al.* [2004]. The resolution for Pn velocity perturbations in most of the TP is about $2.5^\circ \times 2.5^\circ$ (auxiliary material Figure S2). There is also some trade-off between Pn velocity and Pn anisotropy (which is not included in our inversion) [Liang *et al.*, 2004].

3. Inversion Results

3.1. Pn Velocity Variation

[9] Our inversion shows substantial variations in Pn velocity with coherent patterns (Figure 2). The standard errors of Pn velocities yielded from bootstrap inversions are almost all (except for bordering areas) less than 0.05 km/s. Major features are generally consistent with our previous inversion for China [Liang *et al.*, 2004] as outlined below. The increased data coverage and the resolution test (auxiliary material Figure S2) suggest these features are robust.

[10] The major features include the following: (1) Prominent high Pn velocities (8.1 to 8.3 km/s) are found in four major basins bordering the Tibetan and/or Tien Shan (Tarim, Tuha, Qaidam, and Sichuan basins). These basins are tectonically stable with weak deformation and lacking of seismic, thermal, and volcanic activities. Thus, the high Pn velocity anomaly is likely the signature that these basins are strong and cold. (2) The Pn velocity in the western Tien Shan is lower than in the eastern Tien Shan. (3) A high velocity anomaly and a low velocity anomaly are found beneath Bangladesh and eastern India and beneath Myanmar, respectively. Active volcanoes of the region in Myan-

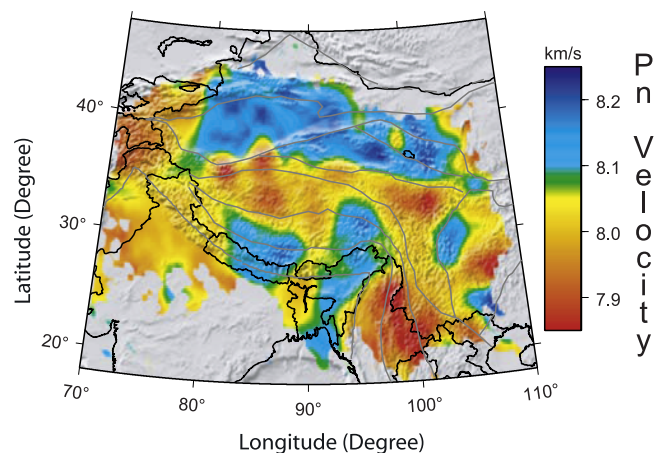


Figure 2. A map of Pn velocity obtained in this study. Major block boundaries are also plotted.

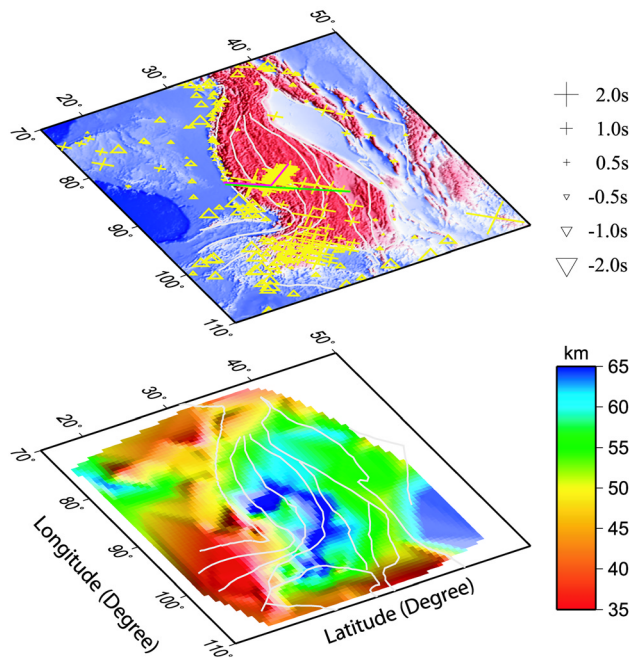


Figure 3. (top) Station delays obtained in this study and (bottom) crustal thickness map inferred from the station delays. The two lines mark the east (green) and west (magenta) profiles of the INDEPTH experiments across the central Tibet.

mar and western Yunnan, China are associated with low Pn velocity. The boundary of the fast and slow anomalies coincides nicely with the India-Eurasia collision zone along the mountain ranges bordering eastern India and Myanmar, suggesting the fast and slow anomalies may be due to strong India lithosphere and weak Eurasia lithosphere as well as the continent-continent collision. (4) Within the Himalayan-Tibetan Plateau, the Pn velocity in northern Tibet is generally lower than that in the south, a well-documented feature as discussed previously. However, our model is more complex, showing significant east-west structures as well. A north-south striking low velocity anomaly is observed to cut through the high velocity southern plateau and extends to India plate. This narrow belt coincides with the location of Yadong-Gulu rift and Yangbajing geothermal on surface, suggesting the surface rifting may have deep root in the mantle.

[11] The most striking feature is the bended low velocity belt (LVB), which extends from west to east beneath northern TP of the Qiangtang block and the Songpan Ganzi fold belt (SGFB) and then turns consistently with the SGFB along eastern TP margin and continues further south to Indo-China. South of Himalayan eastern syntaxis and the Sichuan Basin, the narrow belt expands in east-west direction and occupies almost the whole mountainous regions from Myanmar to western Yangtze Block.

[12] The boundaries of the LVB are well correlated with boundaries at surface separating different geological units. We refer such a boundary as a Pn velocity contrast boundary (VCB). The existence of VCBs suggests strong deformation coupling between crust and, at least uppermost mantle, if not whole lithosphere. The LVB is well delineated by four

prominent VCBs. The most striking VCB is composed of western Altyn Tagh fault (ATF) and Kun Lun fault (KLF), which separate the SGFB to south and Tarim and Qaidam basins, respectively, to north (Figures 1 and 2). The high and low velocity boundary follows nicely along the two faults. The second VCB is Banggong Nujiang suture (BNS), which separates the Lasha block to south and Qiangtang Block to north. The third VCB is composed of three segments, i.e., Longmen thrust fault (LTF), Xianshuihe fault (XF), and southern portion of Red River fault (RRF), from north to south, respectively. This three-segment boundary separates eastern plateau (dominantly low velocity) and western Yangtze Block (dominantly high velocity). In particular, the velocity contrast between eastern plateau and the Sichuan Basin across LTF is as high as 0.3 km/s. The fourth prominent VCB is located along Indo-Myanmar region where the boundary of the fast and slow anomalies coincides approximately with the India-Eurasia collision zone along the mountain ranges bordering eastern India and Myanmar. Notably, the MBT and YZS are not VCBs for Pn velocity.

3.2. Station Delays and Crustal Thickness

[13] As discussed by *Liang et al.* [2004], station delays can be mainly attributed to the crust thickness beneath stations, although crust velocities may need to be taken into account in place where the extreme anomaly exists. Figure 3 shows station delays and a crustal thickness map based on the interpolation of the estimated crustal thickness beneath each station. The crustal thickness is derived from the station delay, assuming the crust velocities from CRUST 2.0 [*Bassin et al.*, 2000]. If the actual average crustal velocity differs by 0.2 km/s, the estimated crustal thickness would have errors of 3.1 km and 4.6 km for a 40 km and 60 km thick crust, respectively. Note the map may have large errors in the areas where there are few stations (western TP, Tarim basin, eastern Sichuan Basin).

[14] The station delays vary considerably (Figure 3, top), ranging from less than -2.0 s to more than 2.0 s. If we attribute all the delays to variation in crustal thickness, one-second delay corresponds to about 10 km difference from the reference model (51 km). The estimated values of crustal thickness (Figure 3, bottom) are: 45–53 km for India Shield, 55–80 km for central TP, 57–69 km for eastern TP margin, and 37–47 km for southeastern TP margin.

[15] Across the India-Himalayan collision zone, the crustal thickness changes rapidly with elevation – the thickness change corresponds to MBT quite well (Figure 3, bottom). The thickest crust is about 75–80 km in south central Tibet (south of YZS in northern Himalaya Block). Across two profiles in central Tibet where we have many PASSCAL stations (Figure 3, top), our estimates generally agree with the results by *Kind et al.* [2002] from receiver function with some discrepancy beneath YZS and BNS (see auxiliary material Figure S3). The crustal thickness increases from about 52 km beneath India to about 76 km south of YZS, then decreases steadily toward north to about 55 km (east line, auxiliary material Figure S3a) or 65 km (west line, auxiliary material Figure S3b) south of BNS. Thus the crust thickness can also vary significantly east-west. In northern TP, the crust remains about 65 km with perhaps thickening

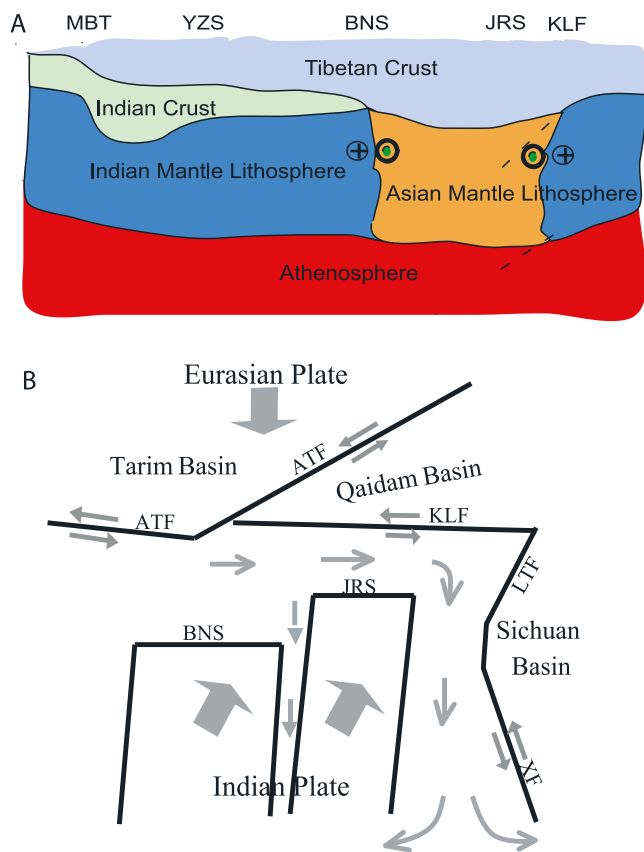


Figure 4. A schematic diagram of the Himalayan-Tibetan collision zone: (a) NS cross-section view, looking to the west, and (b) a map view. The NS cross section in Figure 4a is shown for west-central TP; for the east part of TP, the Indian lithosphere advances further northward.

to 70 km south of JRS. The thickness decreases to 55–60 km north of KF. We see some evidence of crustal thickness change across major boundaries: YYS (by 6 km), BNS (east line) (by 10 km), JRS (by 5 km), and KF (by 7 km). Abrupt change in crustal thickness has been reported across KF [Zhu and Helmberger, 1998] and ATF [Wittlinger *et al.*, 1998].

[16] Our model of crustal thickness is best constrained in the area of eastern and southwestern TP where our station coverage is the best. The crust is thinned rapidly from north to south across the eastern syntaxis latitude, from about 62 km at 28°N (west of Sichuan Basin) to about 33 km at 23°N.

4. Discussion and Conclusion

[17] We presented here a detailed map of Pn velocity variation and estimates of crustal thickness beneath the stations in the TP and surrounding regions. Pn velocity shows a striking LVB, which extends from west to east beneath northern TP to the eastern and southeastern margins of the plateau. The boundaries of the LVB are well correlated with boundaries at surface separating different geological units, suggesting strong deformation coupling between crust and, at least uppermost mantle, if not whole lithosphere.

[18] The low Pn velocity in the northern Tibet correlate with other anomalous observations (inefficient Sn propagation and strong shear-wave anisotropy as discussed previously) and active quaternary volcanism [e.g., Arnaud *et al.*, 1992]. These observations are consistent with the notion that the crust and the lithosphere in the northern TP are hot and deformable. Three mechanisms have been proposed to explain the source of heat: convective removal [Molnar *et al.*, 1993]; subduction-induced upwelling [Tilman and Ni, 2003], and strain heating [McNamara *et al.*, 1994].

[19] Since the collision of India and Eurasia at about 60 Ma, the total north-south convergence is estimated to be 2000–2800 km across western and eastern sectors, among which about 1400 km is taken up within the Himalayan-Tibetan Plateau [Yin and Harrison, 2000; Johnson, 2002]. The mechanism of the crustal thickening in the plateau since the convergence is a matter of great debate. A key question is the extent of underthrusting of India crust and perhaps lithosphere beneath Asia and the amount of shortening of the two plates. A great variety of models have been proposed [e.g., Willet and Beaumont, 1994; Owens and Zandt, 1997; Huang *et al.*, 2000; Johnson, 2002].

[20] Our results are generally consistent with dynamic models that involve with underthrusting in the southern TP, shortening in the northern TP, and extrusion to the east and the southeast (Figure 4). Along the north-south direction, our proposal is similar to earlier models [Owens and Zandt, 1997; Sandvol *et al.*, 1997; Huang *et al.*, 2000] that themselves were synthesized based on available observations at the time. But we envision the dynamic interaction must be 3-dimensional. Beneath the southern Tibet, the Indian crust and rigid lithosphere underthrust Asia crust, giving rise to thickened crust and high Pn velocity. Beneath the northern Tibet, the deformable lithosphere is squeezed by the advancing rigid Indian lithosphere to the south and similarly strong Tarim and Qaidam lithosphere to the north, thus flowing out to the east and turning to the south when meeting the strong Sichuan lithosphere. South of the eastern syntaxis and the Sichuan Basin, the Asian lithosphere spreads out in the southeast direction, where there are no strong confining lithosphere blocks. The pattern of the high and low Pn velocities in the southern TP may suggest that the Indian lithosphere advances further in the eastern part (90–96°E) (to south of JRS) than in the western part (82–90°E) (to south of BNS). The low Pn velocity around 90°E beneath Yadong-Gulu rift zone may suggest extrusion of hot materials from the north.

[21] In this scenario, the thick crust in the northern and eastern TP (although some 10 km thinner than in the Himalayan and southern Tibet) comes from the shortening. The geometry of the crustal thickness in the eastern sector, from thin crust in the southeastern margin and eastern syntaxis to thick crust beneath SGFB and Qiangtang, strongly suggests that the thick crust comes from shortening rather than underthrusting.

[22] The LVB would correlate with the hot and deformable lithosphere in the north, east, and the southeast. GPS measurements suggest that surface deformation changes from east-west direction in the north to south and southeast direction in the eastern margin [Wang *et al.*, 2001]. The fast direction of shear-wave splitting also shows similarly changes from most recent summaries of results [Ni *et al.*,

2006; van der Hilst et al., 2006; Wang et al., 2006]. These observations are also consistent with our suggestion of lithosphere extrusion. It has been suggested that upper crust is decoupled from the lithosphere mantle by partially molten lower crust [Royden et al., 1997]. If this is the case, we argue that the upper crust deformation must be strongly influenced by mantle lithosphere deformation.

[23] **Acknowledgments.** Waveform data were provided by the IRIS DMC and China Earthquake Network Center. We thank Rainer Kind and Xiaohui Yuan for sharing their receiver function results, Wang-Ping Chen for comments on an early version of the manuscript, and Daniel E. McNamara and Xiaohui Yuan for very helpful reviews. Map figures were made using GMT software [Wessel and Smith, 1998].

References

- Arnaud, N. O., P. Vidal, P. Tapponnier, P. Matte, and M. Deng (1992), The high K₂O volcanism of northwestern Tibet: Geochemistry and tectonic implications, *Earth Planet. Sci. Lett.*, *111*, 351–367.
- Barazangi, M., and J. Ni (1982), Velocities and propagation characteristics of Pn and Sn beneath the Himalayan arc and Tibetan Plateau: Possible evidence for underthrusting of Indian continental lithosphere beneath Tibet, *Geology*, *10*, 179–185.
- Bassin, C., G. Laske, and G. Masters (2000), The current limits of resolution for surface wave tomography in North America, *Eos Trans. AGU*, *81*(48), Fall Meet. Suppl., Abstract S12A-03.
- Chen, W. P., and P. Molnar (1981), Constraints on the seismic wave velocity structure beneath the Tibetan Plateau and their tectonic implications, *J. Geophys. Res.*, *86*, 5937–5962.
- Chen, W. P., and S. Ozalaybey (1998), Correlation between seismic anisotropy and Bouguer gravity anomalies in Tibet and its implications for lithospheric structures, *Geophys. J. Int.*, *135*, 93–101.
- Engdahl, E. R., R. van der Hilst, and R. Buland (1998), Global teleseismic earthquake relocation with improved travel times and procedures for depth determination, *Bull. Seismol. Soc. Am.*, *88*, 722–743.
- Hearn, T. M. (1996), Anisotropic Pn tomography in the western United States, *J. Geophys. Res.*, *101*, 8403–8414.
- Hearn, T. M., S. Wang, J. F. Ni, Z. Xu, Y. Yu, and X. Zhang (2004), Uppermost mantle velocities beneath China and surrounding regions, *J. Geophys. Res.*, *109*, B11301, doi:10.1029/2003JB002874.
- Holt, W. E., and T. C. Wallace (1990), Crustal thickness and upper mantle velocities in the Tibetan plateau region from the inversion of regional Pnl waveforms: Evidence for a thick upper mantle lid beneath southern Tibet, *J. Geophys. Res.*, *95*, 12,499–12,525.
- Huang, W., et al. (2000), Seismic polarization anisotropy beneath the central Tibetan Plateau, *J. Geophys. Res.*, *105*, 27,979–27,990.
- Johnson, M. R. W. (2002), Shortening budgets and the role of continental subduction during the India–Asia collision, *Earth Sci. Rev.*, *59*, 101–123.
- Kind, R., et al. (2002), Seismic images of crust and upper mantle beneath Tibet: Evidence for Eurasia plate subduction, *Science*, *298*, 1219–1221.
- Liang, C., X. Song, and J. Huang (2004), Tomographic inversion of Pn travel times in China, *J. Geophys. Res.*, *109*, B11304, doi:10.1029/2003JB002789.
- McNamara, D. E., T. J. Owens, P. G. Silver, and F. T. Wu (1994), Shear wave anisotropy beneath the Tibetan Plateau, *J. Geophys. Res.*, *99*, 13,655–13,665.
- McNamara, D. E., T. J. Owens, and W. R. Walter (1995), Observations of regional phase propagation across the Tibetan Plateau, *J. Geophys. Res.*, *100*, 22,215–22,229.
- McNamara, D. E., W. R. Walter, T. J. Owens, and C. J. Ammon (1997), Upper mantle velocity structure beneath Tibet Plateau from Pn travel time tomography, *J. Geophys. Res.*, *102*, 493–505.
- Molnar, P., P. England, and J. Martinod (1993), Mantle dynamics, uplift of the Tibetan Plateau, and the Indian monsoon, *Rev. Geophys.*, *31*, 357–386.
- Nelson, K. D. (1996), Partially molten middle crust beneath southern Tibet: Synthesis of project INDEPTH initial results, *Science*, *274*, 1684–1687.
- Ni, J., E. Sandvol, and M. West (2006), Seismic anisotropy beneath Tibet and surrounding regions: Implication for the dynamics of the plateau deformation, *Eos Trans. AGU*, *87*(36), West. Pac. Geophys. Meet. Suppl., Abstract S12A-03.
- Owens, T. J., and G. Zandt (1997), Implications of crustal property variations for models of Tibetan Plateau evolution, *Nature*, *387*, 37–43.
- Owens, T. J., G. E. Randall, F. T. Wu, and R. S. Zeng (1993), PASSCAL instrument performance during the Tibet Plateau passive seismic experiment, *Bull. Seismol. Soc. Am.*, *83*, 1959–1970.
- Rapine, R., J. Ni, X. Wu, and T. Hearn (1997), Regional wave propagation in China and surrounding regions, *Bull. Seismol. Soc. Am.*, *87*, 1622–1636.
- Rodgers, A. J., and S. Y. Schwartz (1998), Lithospheric structure of the Qiangtang Terrane, northern Tibetan Plateau, from complete regional waveform modeling: Evidence for partial melt, *J. Geophys. Res.*, *103*, 7137–7152.
- Royden, L. H., et al. (1997), Surface deformation and lower crustal flow in eastern Tibet, *Science*, *276*, 788–790.
- Sandvol, E., J. Ni, R. Kind, and W. Zhao (1997), Seismic anisotropy beneath the southern Himalayas–Tibet collision zone, *J. Geophys. Res.*, *102*, 17,813–17,823.
- Sun, Y., and M. N. Toksöz (2006), Crustal structure of China and surrounding regions from P wave traveltime tomography, *J. Geophys. Res.*, *111*, B03310, doi:10.1029/2005JB003962.
- Tilman, F., and J. Ni (2003), Seismic imaging of the downwelling Indian lithosphere beneath central Tibet, *Science*, *300*, 1424–1427.
- van der Hilst, R., C. Li, H. Yao, Z. Chen, E. Lev, and L. Xu (2006), Crust and upper mantle structure beneath eastern Tibet southwest China: results from MIT-CIGMR broad-band seismometry project, *Eos Trans. AGU*, *87*(36), West. Pac. Geophys. Meet. Suppl., Abstract S41A-0164.
- Wang, C., P. Silver, L. Zhu, and W. Chan (2006), Seismic experiment along 30° in the east Tibetan and west Sichuan, China, *Eos Trans. AGU*, *87*(36), West. Pac. Geophys. Meet. Suppl., Abstract S41A-0162.
- Wang, Q., et al. (2001), Present-day crustal deformation in China constrained by global positioning system measurements, *Science*, *294*, 574–577.
- Wessel, P., and W. H. F. Smith (1998), New, improved version of the Generic Mapping Tools released, *Eos Trans. AGU*, *79*(47), 579.
- Willet, S. D., and C. Beaumont (1994), Subduction of Asian lithospheric mantle beneath Tibet inferred from models of continental collision, *Nature*, *369*, 642–645.
- Wittlinger, G., et al. (1998), Tomographic evidence for localized lithospheric shear along the Altyn Tagh fault, *Science*, *282*, 74–76.
- Yin, A., and T. M. Harrison (2000), Geological evolution of the Himalayan–Tibetan orogen, *Annu. Rev. Earth Planet. Sci.*, *28*, 211–280.
- Zhao, L. S., and J. K. Xie (1993), Later variation in compressional velocities beneath the Tibetan Plateau from Pn traveltime tomography, *Geophys. J. Int.*, *115*, 1070–1084.
- Zhu, L., and D. Helmberger (1998), Moho offset across the northern margin of the Tibetan Plateau, *Science*, *281*, 1170–1172.

C. Liang, Center for Earthquake Research and Information, University of Memphis, 3892 Central Avenue, Memphis, TN 38152, USA. (cliang1@memphis.edu)

X. Song, Department of Geology, University of Illinois at Urbana-Champaign, 1301 W Green Street, Urbana, IL 61801, USA. (xsong@uiuc.edu)